

Display Technology Letters

Sunlight Readable Fast-Response Transflective LCDs by Horizontal Electric Fields

Meizi Jiao and Shin-Tson Wu, *Fellow, IEEE*

Abstract—Two single-cell-gap transflective display devices with vertically aligned positive dielectric anisotropy liquid crystal driven by horizontal electric fields are proposed. In these displays, patterned reflectors are located at transmittance-inefficient regions to serve as reflective mode. These displays exhibit fast response time, high transmittance, and wide view with optical compensation. Potential applications of these displays for sunlight readable mobile devices are emphasized.

Index Terms—Fast response, liquid crystal displays (LCDs), single cell gap, sunlight readability.

I. INTRODUCTION

SUNLIGHT readability is an important requirement for mobile displays such as digital cameras, portable video players and cellular phones because of their outdoor applications. Moreover, fast response is highly desirable because many mobile devices are used to play movies and videos. To display fast moving pictures without causing noticeable image blurs, a response time below ~ 3 ms is required. To satisfy sunlight readability, various single-cell-gap and dual-cell-gap transflective liquid crystal displays (TR-LCDs) have been proposed [1], [2]. Among these two, the single-cell-gap approach is more favorable because it is easier to fabricate, however, it is more difficult to match the phase retardation between transmissive (T) region and reflective (R) region than the dual-cell-gap one. Several approaches for improving the response time of a TR-LCD have also been proposed [3]–[5]. However, technical challenges for fabricating such devices remain to be overcome. For example, the dual fringing field switching mode [5], [6] offers a fast response time, but horizontal alignment accuracy between top and bottom electrodes is a big concern.

In this letter, we propose a sunlight readable fast-response TR-LCD using vertically aligned positive dielectric anisotropy ($\Delta\epsilon > 0$) liquid crystal (LC) driven by a horizontal electric field generated by fringing field switching (FFS) [7] or in-plane switching (IPS) [8], [9] electrodes. Such modes [8], [10] usually exhibit a low transmittance in T-mode because there are some

Manuscript received December 30, 2009. Current version published March 31, 2010.

The authors are with the College of Optics and Photonics, University of Central Florida, Orlando, FL 32816 USA (e-mail: mjiao@mail.ucf.edu, swu@mail.ucf.edu).

Color versions of one or more of the figures in this paper are available online at <http://ieeexplore.ieee.org>.

Digital Object Identifier 10.1109/JDT.2010.2043214

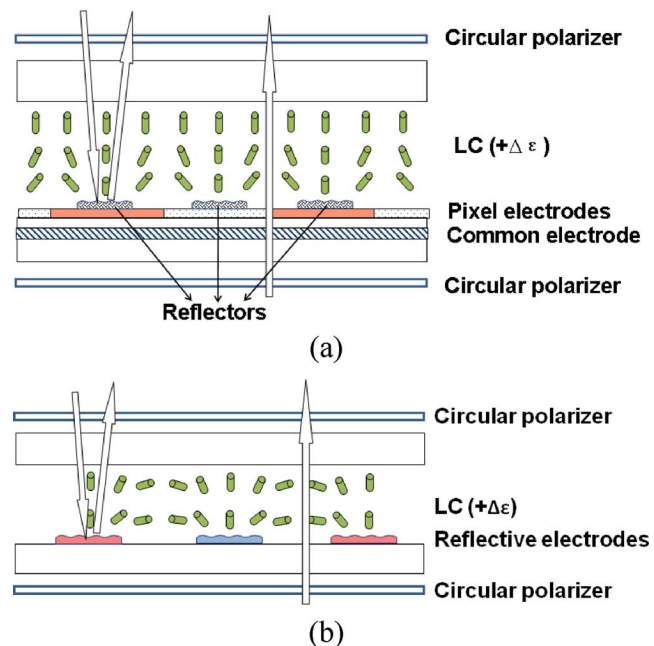


Fig. 1. Schematic structure of the sunlight readable TR-LCDs using a positive $\Delta\epsilon$ LC driven by horizontal electric fields generated by: 1) FFS electrodes and 2) IPS electrodes.

low transmittance areas or even dead zones due to non-uniform distribution of horizontal electric fields. In the present design, we embed reflectors under these low transmittance areas so that they function as R-region. The double pass of the ambient light improves the reflectance. Two TR-LCD modes are proposed based on this concept. The first one uses FFS electrodes and the second uses IPS electrodes. Both designs show good sunlight readability, high transmittance, fast response time, and wide viewing angle with a proper phase compensation [11]–[13].

II. DEVICE CONFIGURATIONS

Fig. 1 shows a cross-section of the schematic structure of the proposed TR-LCDs, using: 1) FFS electrodes and 2) IPS electrodes. In both displays, the LC cell is sandwiched between two circular polarizers. The employed LC has a positive $\Delta\epsilon$ and is vertically aligned, resulting in a normally black state under crossed circular polarizers. The driving electrodes are located at the inner side of the bottom substrate.

The structure with FFS electrodes shown in Fig. 1(a) has patterned pixel electrodes and a plane common electrode located below. In a voltage-on state, fringing electric fields are

generated between pixel electrodes and common electrode. The LC directors are reoriented as shown in Fig. 1(a). The horizontal field is the strongest near the edges of pixel electrodes where effective domains are formed. While at the centers of electrodes and gaps, LC remains vertical because the horizontal electric field component is too weak to reorient the LC directors. Therefore the phase retardation is small which leads to a low transmittance or dead zones in the T mode. Here we embedded patterned bumpy reflectors in these areas. In the R-mode, the ambient light traverses the LC layer twice, so the optical phase retardation is doubled and reflectance improved. Meanwhile, the transmittance in the T-region is also enhanced because the low transmittance areas are now used as reflective mode.

The working principle is similar for the structure with IPS electrodes shown in Fig. 1(b). However, the pixel electrodes and common electrodes in IPS cell are both patterned and located alternately to each other. In this case, the inefficient regions are formed coincident with driving electrodes locations. So instead of inserting an extra layer of patterned reflectors, we use reflective electrodes to achieve reflective regions. As a result, both sunlight readability and high transmittance are achieved without complicated fabrication process.

III. RESULT

The proposed TR-LCD structures are optimized using a three-dimensional LC simulator (TECHWIZ developed by Sanayi). The LC distribution is calculated by the finite-element method [14] and the optical properties are calculated based on extended 2×2 Jones matrix methods [15], [16].

In order to obtain fast response time, narrow electrode width and gap are preferred. With smaller electrode dimension, the generated electric field is stronger, and smaller effective sub-domains can be formed. Both factors help reduce the response time. On the other hand, it is very difficult to fabricate too narrow electrodes arrays. Balancing both sides, we used electrode width $W = 3 \mu\text{m}$ and gap $G = 4 \mu\text{m}$ in both FFS and IPS cells as Fig. 1 shows. The penetration depth of fringing field into LC cell is quite shallow with such electrode dimension. In this case, high birefringence (Δn) LC material is needed in order to accumulate enough phase retardation. In the FFS cell shown in Fig. 1(a), we used UCF-2 type high Δn LC [17] with following parameters: $K_{11} = 17.3 \text{ pN}$, $K_{22} = 10.4 \text{ pN}$, $K_{33} = 28.3 \text{ pN}$, $\Delta n = 0.416$, dielectric anisotropy $\Delta \epsilon = 18.27$, and rotational viscosity $\gamma_1 = 200 \text{ mPa} \cdot \text{s}$. While in IPS cell shown in Fig. 1(b), the LC material parameters are as follows: $K_{11} = 12 \text{ pN}$, $K_{22} = 9 \text{ pN}$, $K_{33} = 20 \text{ pN}$, $\Delta n = 0.2$, $\Delta \epsilon = 11$, and $\gamma_1 = 250 \text{ mPa} \cdot \text{s}$.

Fig. 2 depicts the normalized voltage-dependent transmittance (VT) and voltage-dependent reflectance (VR) curves of the proposed TR-LCD with a) FFS electrodes and b) IPS electrodes at wavelength $\lambda = 550 \text{ nm}$. Since T-part uses a backlight while R-part uses ambient light to display images, we should compare the normalized VT and VR curves instead of their absolute values. In the FFS structure, both cell gap and reflector width are optimized to obtain matched VT and VR curves. Here, cell gap d is $4 \mu\text{m}$ and reflector width W_r is $1.6 \mu\text{m}$ locating at the pixel electrodes center and gap center. From Fig. 2(a), the VT and VR curves of the FFS-based TR-LCD match with

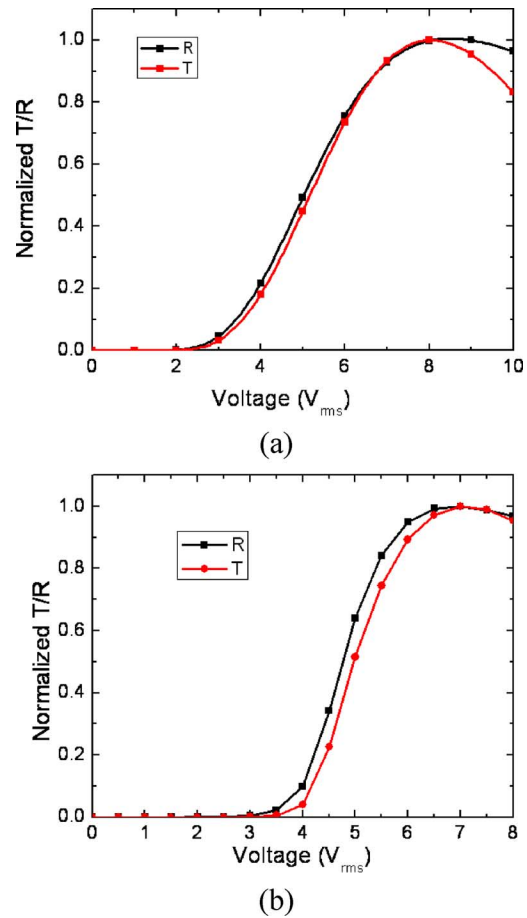


Fig. 2. Normalized VT and VR curves of the proposed sunlight readable TR-LCDs with (a) FFS electrodes and (b) IPS electrodes at $\lambda = 550 \text{ nm}$.

each other very well so that a single gamma curve can be used. The peak transmittance ($\sim 89\%$) normalized to that of two paralleled linear polarizers (37%) occurs at $V_{\text{on}} = 8 V_{\text{rms}}$, and the reflectance is $\sim 46\%$. Fig. 2(b) shows the VT and VR curves of the IPS-based TR-LCD. Since reflective electrodes are used in this cell instead of extra reflectors, reflector width is determined by the driving electrodes width. Therefore only cell gap can be optimized to match VT and VR curves. With an optimized cell gap $d = 3 \mu\text{m}$, although VT and VR curves are not matched with each other so well as in the FFS cell, it is still fairly good for single gamma driving. At $V_{\text{on}} = 7 V$, the transmittance reaches $\sim 85\%$ while reflectance $\sim 42\%$. In both cells, the low reflectance originates from dead zones at the center of reflectors. However, sunlight readability is essential only when the device is used under strong ambient light. In this case, the luminance in R-part is still quite large due to strong ambient light. Together with antireflection film, good sunlight readability can be achieved.

The response time (10%-90% transmittance change) of the proposed TR-LCDs are calculated as plotted in Fig. 3(a) for the FFS electrodes and Fig. 3(b) for the IPS electrodes. The rise time and decay time for the FFS structure [Fig. 1(a)] are $\sim 1.19 \text{ ms}$ and $\sim 1.43 \text{ ms}$ for T-part, and $\sim 2.09 \text{ ms}$ and $\sim 2.07 \text{ ms}$ for R-part, respectively. While for the IPS structure [Fig. 1(b)], they are $\sim 5.99 \text{ ms}$ and $\sim 5.58 \text{ ms}$ for T-part, and $\sim 8.39 \text{ ms}$ and

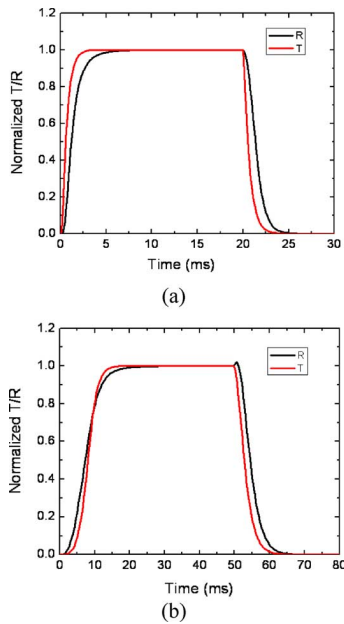


Fig. 3. Simulated response times for the proposed sunlight readable TR-LCDs: (a) with FFS electrodes and (b) with IPS electrodes.

TABLE I
SIMULATED GTG RESPONSE TIME (MS) FOR THE T-PART [FIG. 1(A)].

	1	2	3	4	5	6	7	8
1		5.54	4.51	3.86	3.45	2.91	2.47	1.19
2	1.04		3.15	2.68	2.42	2.07	1.77	0.80
3	1.05	2.92		2.47	2.21	1.93	1.67	0.71
4	1.07	2.57	2.54		2.08	1.87	1.62	0.65
5	1.10	2.43	2.36	2.12		1.86	1.61	0.61
6	1.16	2.34	2.31	2.17	2.03		1.58	0.53
7	1.22	2.34	2.34	2.24	2.14	1.80		0.44
8	1.43	2.57	2.65	2.62	2.58	2.41	2.30	

TABLE II
SIMULATED GTG RESPONSE TIME (MS) FOR THE R-PART [FIG. 1(B)].

	1	2	3	4	5	6	7	8
1		5.69	4.95	4.49	4.17	3.69	3.28	2.09
2	1.79		3.93	3.71	3.49	3.10	2.77	1.73
3	1.85	3.67		3.43	3.32	3.00	2.70	1.68
4	1.90	3.63	3.23		3.21	2.98	2.70	1.68
5	1.94	3.59	3.39	2.92		3.02	2.73	1.72
6	2.00	3.57	3.48	3.26	3.06		2.72	1.81
7	2.05	3.58	3.54	3.38	3.24	2.69		1.95
8	2.07	3.59	3.64	3.56	3.50	3.27	3.34	

~ 6.46 ms for R-part, respectively. Both devices exhibit a fairly fast response time. Especially the FFS-based TR-LCD shows a fast gray-to-gray (GTG) response time without an overdrive or undershoot voltage [18]. We divided the VT curve uniformly into eight gray levels (1–8) and calculated the response time between each gray level. Tables I and II list the calculated GTG response times of the structure shown in Fig. 1(a) for T- and R-parts, respectively. The averaged response time is ~ 2.08 ms for T-part and ~ 3.10 ms for R-part. The fast response time

makes this TR-LCD attractive for mobile devices with video applications and color sequential displays [19].

IV. CONCLUSION

We have proposed two sunlight readable TR-LCDs driven by FFS and IPS electrodes, respectively. With single cell gap, the proposed structures exhibit a high transmittance and matched VT and VR curves for single gamma driving. Both structures show fast response and especially the one with FFS electrodes shows fast GTG response without overdrive or undershoot approaches. Moreover, these devices do not require any rubbing nor complicated fabrication processes. Therefore, their application for mobile displays is foreseeable.

REFERENCES

- [1] X. Zhu, Z. Ge, T. X. Wu, and S. T. Wu, "Transflective liquid crystal displays," *J. Display Technol.*, vol. 1, no. 1, pp. 15–29, Sep. 2005.
- [2] A. K. Bhowmik, Z. Li, and P. J. Bos, *Mobile Displays: Technology and Applications*. New York: Wiley, 2008.
- [3] J. H. Lee, X. Zhu, and S. T. Wu, "Novel color-sequential transflective liquid crystal displays," *J. Display Technol.*, vol. 3, no. 1, pp. 2–8, Mar. 2007.
- [4] I. A. Yao, H. L. Ke, C. L. Yang, C. J. Chen, J. P. Pang, T. J. Chen, and J. J. Wu, "Electrooptics of transflective displays with optically compensated bend mode," *Jpn. J. Appl. Phys.*, vol. 45, pp. 7831–7836, 2007.
- [5] M. Jiao, S. T. Wu, and W. K. Choi, "Fast-response single cell gap transflective liquid crystal displays," *J. Display Technol.*, vol. 5, no. 3, pp. 83–85, Mar. 2009.
- [6] M. Jiao, Z. Ge, S. T. Wu, and W. K. Choi, "Submillisecond response nematic liquid crystal modulators using dual fringe field switching in a vertically aligned cell," *Appl. Phys. Lett.*, vol. 92, p. 111101, 2008.
- [7] S. H. Lee, S. L. Lee, and H. Y. Kim, "Electro-optic characteristics and switching principle of a nematic liquid crystal cell controlled by fringe-field switching," *Appl. Phys. Lett.*, vol. 73, pp. 2881–2883, 1998.
- [8] R. A. Soref, "Field effects in nematic liquid crystals obtained with interdigital electrodes," *J. Appl. Phys.*, vol. 45, p. 5466, 1974.
- [9] M. Oh-e and K. Kondo, "Electro-optical characteristics and switching behavior of the in-plane switching mode," *Appl. Phys. Lett.*, vol. 67, pp. 3895–3897, 1995.
- [10] S. H. Hong, Y. H. Jeong, H. Y. Kim, H. M. Cho, W. G. Lee, and S. H. Lee, "Electro-optic characteristics of 4-domain vertical alignment nematic liquid crystal display with interdigital electrode," *J. Appl. Phys.*, vol. 87, pp. 8259–8263, 2000.
- [11] R. Lu, X. Zhu, S. T. Wu, Q. Hong, and T. X. Wu, "Ultrawide-view liquid crystal displays," *J. Display Technol.*, vol. 1, no. 1, pp. 3–14, Sep. 2005.
- [12] Z. Ge, R. Lu, T. X. Wu, C. L. Lin, N. C. Hsu, W. Y. Li, and C. K. Wei, "Extraordinarily wide-view circular polarizers for liquid crystal displays," *Opt. Express*, vol. 16, pp. 3120–3129, 2008.
- [13] X. Zhu, Z. Ge, and S. T. Wu, "Analytical solutions for uniaxial-film-compensated wide-viewing liquid crystal displays," *J. Display Technol.*, vol. 2, no. 1, pp. 2–20, Mar. 2006.
- [14] Z. Ge, T. X. Wu, R. Lu, X. Zhu, Q. Hong, and S. T. Wu, "Comprehensive three-dimensional dynamic modeling of liquid crystal devices using finite element method," *J. Display Technol.*, vol. 1, no. 2, pp. 194–206, Dec. 2005.
- [15] A. Lien, "Extended Jones matrix representation for the twisted nematic liquid-crystal display at oblique incidence," *Appl. Phys. Lett.*, vol. 57, pp. 2767–2769, 1990.
- [16] Z. Ge, T. X. Wu, X. Zhu, and S. T. Wu, "Reflective liquid crystal displays with asymmetric incidence and exit angles," *J. Opt. Soc. Am. A.*, vol. 22, pp. 966–977, 2005.
- [17] S. Gauza, H. Wang, C. H. Wen, S. T. Wu, A. J. Seed, and R. Dabrowski, "High birefringence isothiocyanato tolane liquid crystals," *Jpn. J. Appl. Phys.*, vol. 42, pp. 3463–3466, 2003.
- [18] S. T. Wu and C. S. Wu, "High-speed liquid-crystal modulators using transient nematic effect," *J. Appl. Phys.*, vol. 65, pp. 527–532, 1989.
- [19] S. Gauza, X. Zhu, W. Piecek, R. Dabrowski, and S. T. Wu, "Fast switching liquid crystals for color-sequential LCDs," *J. Display Technol.*, vol. 3, no. 3, pp. 250–252, Sep. 2007.